Biochimica et Biophysica Acta 1810 (2011) 867–874

Contents lists available at ScienceDirect

Biochimica et Biophysica Acta

journal homepage: www.elsevier.com/locate/bbagen

The significance of chloride in the inhibitory action of disodium cromoglycate on immunologically-stimulated rat peritoneal mast cells

J.K.Y. Law [a], C.K. Yeung [b,*], S.P. Wan [b], S. Ingebrandt [c], H.Y.A. Lau [b], J.A. Rudd [b], M. Chan [a]

[a] Bioengineering Graduate Programme, The Hong Kong University of Science and Technology (HKUST), Clear Water Bay, Hong Kong
[b] The School of Biomedical Sciences, Faculty of Medicine, The Chinese University of Hong Kong (CUHK), Shatin, Hong Kong
[c] Department of Informatics and Microsystem Technology, University of Applied Sciences Kaiserslautern, D-66482 Zweibrücken, Germany

ARTICLE INFO

Article history:
Received 17 December 2010
Received in revised form 9 May 2011
Accepted 13 May 2011
Available online 23 May 2011

Keywords:
Chloride
Anti-IgE
Rat peritoneal mast cells
Disodium cromoglycate
Histamine
Extracellular electrophysiology

ABSTRACT

Background: The microelectrode array (MEA) was used to investigate the pharmacological relevance of chloride (Cl^-) ions in antigen-dependent mast cell activation and the inhibitory effect of disodium cromoglycate (DSCG) on mast cell activation.
Methods: The movements of ions across the cellular membrane and the potential relationship between Cl^- channels and DSCG during immunological activation were investigated using the MEA. The results were then subsequently compared with the amount of histamine released from anti-IgE activated peritoneal mast cells.
Results: The inclusion of charybdotoxin (ChTX) in Cl^--free buffer showed that the measured field potentials during antigen-stimulated peritoneal mast cell were a combination of Cl^- influx and K^+ efflux. The delayed onset time of Cl^- influx indicated the presence of a delayed outwardly-rectifying Cl^- current in the antigen-stimulated peritoneal mast cells. The use of 5-nitro-2-(3-phenylpropylamino) benzoic acid demonstrated that the activated mast cell membrane potential can be stabilised, thereby reducing the amount of histamine released from the anti-IgE activated mast cells. The correlation between the results of the histamine release assay and the electrophysiological measurements demonstrated the importance of Cl^- to anti-IgE dependent mast cell activation. The inhibitory effect of DSCG on anti-IgE activated cells, however, did not correlate with the presumed influx of Cl^-.
Conclusions: The MEA data suggest that Cl^- influx is crucial to IgE-dependent mast cell degranulation.
General significance: While the MEA cannot yield information about single channel properties, it is convenient to use and can provide information on the global changes in electrophysiological responses of non-excitable cells.

1. Introduction

Immunoglobulin E (IgE)-dependent mast cell activation is a major triggering mechanism for both acute and chronic allergic reactions [1,2]. In response to IgE-dependent activation, high-affinity cell surface receptors (FcεRI) on mast cell surface are aggregated. The downstream signalling pathways responsible for cytokine production and mast cell degranulation are subsequently activated [3]. It is well known that mast cell activation is intricately regulated by the intracellular calcium concentration $[Ca^{2+}]_i$ as well as the influx of Ca^{2+} [2]. The aggregation of FcεRI translocates Ca^{2+} from internal stores to the cytoplasm and elevates the amount of $[Ca^{2+}]_i$. This increase in $[Ca^{2+}]_i$ opens Ca^{2+} channels in the plasma membrane to facilitate further Ca^{2+} influx [4]. The opened Ca^{2+} channels are known as calcium-release activated calcium channels (CRAC), and the corresponding Ca^{2+} selective current is termed I_{CRAC} [5].

Apart from Ca^{2+}, flow of other ions such as potassium (K^+) and chloride (Cl^-) are likely to play equally important roles in mast cell activation. Studies have revealed that mediators released from activated mast cells can be potentiated by extracellular concentrations of K^+ or Cl^- [6–9]; and that K^+ and Cl^- channel blockers are able to reduce the degranulation process [10–13]. The signalling mechanism probably involves secondary diffusible messengers that empty the internal Ca^{2+} store and thus favours the influx of Ca^{2+} [14].

Chloride channel subtypes are found in both human and rodent mast cells [15,16]. A moderately outwardly-rectifying Cl^- current (I_{ORCC}) has been detected in both resting and antigen-stimulated rat peritoneal mast cells [17,18]. The delayed I_{ORCC} can be induced by the elevation of intracellular second messenger cyclic AMP (cAMP), which influences Ca^{2+} influx in activated mast cells by mechanisms that are yet to be elucidated [18,19]. The delayed onset of cAMP-induced I_{ORCC} suggests the cAMP effect on Cl^- conductance is indirect and that a

Abbreviations: MEA, microelectrode array; sodium cromoglycate, DSCG; delayed outwardly-rectifying chloride channel, I_{ORCC}; calcium-release activated calcium channel, CRAC; charybdotoxin, ChTX; calcium-dependent potassium channel, K_{Ca} channel

* Corresponding author at: Room 405L, Basic Medical Sciences Building, The School of Biomedical Sciences, Faculty of Medicine, The Chinese University of Hong Kong (CUHK), Shatin, Hong Kong. Tel.: +852 9533 2699; fax: +852 2603 5139.
E-mail address: yeungck@rocketmail.com (C.K. Yeung).

0304-4165/$ – see front matter © 2011 Elsevier B.V. All rights reserved.
doi:10.1016/j.bbagen.2011.05.007

phosphorylation process by a cAMP-dependent protein kinase may be involved [20]. Besides cAMP, G-proteins may be involved in the development of I_{ORCC} since internal guanosine 5′-O-(3-thiotriphosphate) is able to trigger this current [18]. It is believed that the delayed Cl^- conductance maintains cell membrane hyperpolarisation and promotes Ca^{2+} influx during mast cell activation. Inhibition of Cl^- channel activity and inflammatory mediators have been observed with either 5-nitro-2-(3-phenylpropylamino) benzoic acid (NPPB), a potent Cl^- channel blocker; or cromolyn, a mast cell stabiliser, in rat mucosal-type mast cells [13].

Disodium cromoglycate (DSCG) has been used extensively as an anti-allergic drug, and a study has illustrated that it may indirectly prevent the influx of Ca^{2+} by blocking the Cl^- channels [21]. Using the microelectrode array (MEA) as a detection tool, the present study used K^+ and Cl^- channel blockers to further characterise the pharmacological relevance of Cl^- ions in antigen-dependent mast cell activation and the inhibitory effect of DSCG on mast cell activation. A functional histamine release assay was used to investigate if the field potential measurements obtained using the MEA correlated with extracellular histamine levels. In order to identify the role of Cl^- during activation, the relationship between Ca^{2+} influx and in the presence or absence of Cl^- was further analysed using the Fura-2 fluorometric technique.

2. Materials and methods

2.1. Animals

Male Sprague–Dawley (SD) rats, weighing 250–300 g, were sensitised by a single intraperitoneal injection of a 0.5 ml emulsion containing ovalbumin (60 mg/ml), aluminium hydroxide (240 mg/ml), and pertussis vaccine (1.33 i.u./ml) in 0.01 M phosphate-buffered saline 7–8 weeks before obtaining the peritoneal mast cells for the experiments. The rats were outbred within the Laboratory Animal Services Centre of the Chinese University of Hong Kong and were housed at approximately 25 °C in 12-hour light/dark cycles. The Animal Experimentation Ethics Committee, the Chinese University of Hong Kong, approved the experiments and protocols used.

2.2. Preparations of media

2.2.1. Standard buffer

The standard buffer (pH 7.4) contained (mM): NaCl (137), glucose (5.6), *N*-2-hydroxyethylpiperazine-*N*′-2-ethanesulphonic acid (HEPES, 10), KCl (2.7), NaH_2PO_4 (0.4), and $CaCl_2$ (1.0).

2.2.2. Low chloride and chloride-free buffers

The isethionate buffer (low Cl^-) contained (mM): $C_2H_5O_4SNa$ (137), KCl (2.7), $NaH_2PO_4{\cdot}2H_2O$ (0.4), $CaCl_2$ (1.0), HEPES (10), and Glucose (5.6). This buffer was used in the low Cl^- experiments.

The gluconate buffer (Cl^--free) contained (mM): $NaC_6H_{11}O_7$ (137), $KC_6H_{11}O_7$ (2.7), $NaH_2PO_4{\cdot}2H_2O$ (0.4), $Ca(C_6H_{11}O_7)_2$ (1.0), HEPES (10), and Glucose (5.6). This buffer was used in the Cl^--free experiments.

2.2.3. Chloride-free buffer containing charybdotoxin (ChTX)

The Cl^--free buffer containing ChTX (100 nM), which blocks the Ca^{2+}-dependent K^+ (K_{Ca}) channels, was used in the MEA signal verification experiments.

2.3. Preparation of peritoneal mast cells

SD rats were sacrificed by decapitation, followed by exsanguination under running water. A 25 ml volume of heparin (50 IU/ml)-containing standard buffer was injected into the SD rat intraperitoneally. The solution-filled peritoneal cavity was then gently lavaged for 2 min. The injected buffer (containing approximately 4–5% peritoneal mast cells at this point) was extracted and centrifuged (180*g* at 4 °C for 5 min).

After discarding the supernatant, the cells were resuspended in standard buffer supplemented with bovine serum albumin (BSA, 1 mg/ml). Rat peritoneal mast cells were isolated and purified using a Percoll ® density gradient. The cell suspension (1 ml) was mixed with 4 ml of 90% Percoll®, and 1 ml of BSA-supplemented standard buffer was then carefully layered onto the Percoll®-cell mixture. Purification was performed by centrifugation (150*g* at 4 °C for 25 min), which allowed cell separation and gradient formation simultaneously. Peritoneal mast cells would gather as a single layer at the bottom of the tube, whereas other cells would form a rather compact layer on top of the gradient. The peritoneal mast cell pellet was then collected and washed once in standard buffer and once in the corresponding buffer by centrifugation (180*g* at 4 °C for 5 min) before resuspending the cells at the desired density in the corresponding buffer. The peritoneal mast cell purity of >98% was confirmed with toluidine blue staining.

2.4. Microelectrode arrays

The MEAs were manufactured on glass wafers (Borofloat 33, SCHOTT GLAS, Mainz, Germany) using standard silicon technology. The planar 64-channel gold microelectrode arrays (8×8) with a diameter of 20 μm and at a pitch of either 100 or 200 μm were used. In order to use the MEA several times, the chip surface was passivated by an oxide-nitride-oxide layer deposited by plasma enhanced chemical vapour deposition consisting of 500 nm SiO_2, 500 nm Si_3N_4, and 100 nm SiO_2. Details of the fabrication and encapsulation processes have been described [22,23].

A custom-made 64-channel amplifier system, in which microelectrodes were coupled directly to the inputs of high impedance operational amplifiers, (OPA 627, input impedance $Z_{in}=14$ TΩ, gain: 33×; Burr-Brown, Texas Instruments, Dallas, Texas 75265, USA) was used. This was then coupled to a main amplifier (gain: 33×), providing an overall gain of 1089×. Data were sampled at 10 kHz per channel, with simultaneous acquisition across all channels (PCI 6071E, National Instruments, Hong Kong) using MED64 conductor 3.1 software (Alpha MED Sciences Co. Ltd., Japan). An extracellular Ag/AgCl electrode, which was set to ground potential, served as a reference electrode. A more detailed description of the data acquisition has been published previously [22,23].

2.5. Chemicals and reagents

Percoll© was purchased from GE healthcare bioscience, Uppsala, Sweden for gradient-purification. Sheep anti-rat IgE was purchased from MP Biomedicals, Germany, and NPPB was purchased from Tocris Bioscience, USA. Disodium cromoglycate (DSCG), dimethylsulfoxide (DMSO), BSA, Fura-2 acetoxymethyl ester (AM), and all other chemicals of analytical grade were purchased from Sigma-Aldrich, St. Louis, MO, USA. The stock of sheep anti-rat IgE, ChTX, and DSCG were made using distilled water. The stock of NPPB and Fura-2 AM were made using DMSO. Subsequent dilutions were made using the appropriate buffer.

2.6. Experimental procedures

2.6.1. Histamine release assay

Peritoneal mast cells were suspended and equilibrated in 450 μl of corresponding test buffers or standard buffer with NPPB or DSCG at 37 °C for 0 min or 10 min before the addition of 50 μl of 10× anti-IgE (1/5,000 to 1/100) for activation. The histamine release reaction was stopped by adding 1 ml ice cold buffer 10 min later. The amount of histamine released from the antigen-stimulated cells was then

quantified spectrofluorometrically using a Histamine AutoAnalyzer 3 system from Bran + Luebbe GmbH (Norderstedt, Germany). The results were calculated as a percentage of the total histamine content released by the cells into the supernatant following exposure to anti-IgE:

$$\text{Histamine release } (\%) = [S \div (S + C)] \times 100\%$$

where S = amount of histamine released into the supernatant, C = amount of histamine remaining in the cell pellet.

All results were corrected for the amount of histamine spontaneously released into the supernatant when incubated in buffer alone (less than 5% of total cellular histamine in general).

2.6.2. Electrophysiological measurements

Peritoneal mast cells were resuspended at a cell density of approximately 3×10^6 cells/ml in the corresponding buffers. A cell suspension of 33 μl (about 10^5 cells) was placed onto the recording area of the MEA. The chips, about 15 of them from each culture, were then incubated at 37 °C balanced with 5% CO_2 for at least 15 min. They were then transferred to the headstage amplifier followed by adding 157 μl corresponding buffer with or without NPPB or DSCG. In experiments studying the effects of anti-IgE on peritoneal mast cells, a *bolus dose* of 10 μl was delivered by a micro-syringe to give a final MEA volume of 200 μl (i.e. 33 μl cell suspension + 157 μl corresponding buffer with or without NPPB or DSCG + 10 μl drug). In experiments studying the blocking effects of NPPB and DSCG on peritoneal mast cells, cells were either pre-incubated in the drug-containing buffer for 0 min or 10 min before 10 μl of anti-IgE was added. The final concentrations of anti-IgE (1/50,000 to 1/100) were chosen as they are comparable to the concentrations used in other studies. For the controls, adding 10 μl drug-free standard buffers to cell-containing MEAs or injecting 10 μl drug-containing standard buffers to cell-free MEAs was performed in order to determine whether electrophysiological signals were generated by either the injection technique or the presence of drug.

2.6.3. Intracellular Ca^{2+} measurements

A suspension containing 10^6 cells/ml of Percoll® purified rat peritoneal mast cells was prepared as described in the previous section. The cells were loaded with 1 μM of Fura-2 AM in BSA-standard buffer for 20 min at 37 °C with occasional agitation. The cell suspension was then diluted 3 fold using prewarmed BSA-supplemented standard buffer and was left for 5–10 min at 37 °C for the complete hydrolysis of ester to free acid. The unbound dye was then removed by centrifugation (12,000*g* at 25 °C for 30 sec). The cells were kept at 4 °C following re-suspension in 500 μl buffer, and they were used within 90 min as leakage of the dye tends to occur over time.

The Fura-2 AM fluorescence-bound intracellular Ca^{2+} was measured using a Mira*Cal* PRO ratio imaging system from Life Science (Cambridge, UK). Mira*Cal* PRO consists of a SpectraMASTER monochromatic illuminator, a high resolution integrating video camera supporting a resolution of up to 768 × 576 pixels, a *Lecia* fluorescence microscope equipped with a temperature controlled perfusion chamber, and a personal computer with a Windows 95 based system control processor. For every measurement, 5 μl of the Fura-2 loaded cell suspension was added to the centre of a coverslip, which was held inside a metal chamber. The chamber was kept at 37 °C by a heater and 500 μl of prewarmed buffer was then added to the cells after 60 sec. A volume of 500 μl of anti-IgE (1/100 dilution) was added to the cells at 50 s, giving a final bath dilution of 1/200. The cells in the chamber were excited cyclically by wavelengths of 340 nm and 380 nm while the fluorescence signals at the emission wavelength of 510 nm were recorded every 0.8 sec for 5 min. All readings were adjusted against background fluorescence signals at the two excitation wavelengths. The intracellular Ca^{2+} was automatically calculated by Life Science MiraCal software version 1.8 software using the Grynkiewicz equation [24]:

$$\left[Ca^{2+}\right] = K_d \beta \times (R - R_{min}) / (R_{max} - R)$$

where K_d = dissociation constant for the dye (224 nM for fura-2/Ca^{2+} complex at 37 °C and pH 7.0), R = ratio of fluorescence signal at 340 nm to fluorescence signal at 380 nm measured at 510 nm emission wavelength, R_{min} = ratio of fluorescence when the dye is completely free of Ca^{2+}, R_{max} = ratio of fluorescence when the dye is saturated with Ca^{2+}, and β = ratio of saturated fluorescence to free fluorescence at 380 nm excitation.

The parameters of the above equation were determined by measuring the fluorescence signals of Fura-2 free acid in Ca^{2+} saturated (5 mM $CaCl_2$ solution) and in Ca^{2+}-free ($CaCl_2$-free solution with 5 mM EGTA) conditions at wavelengths of 340 nm or 380 nm with emission at 510 nm. Results were expressed as an increase in free intracellular [Ca^{2+}] (nM) over the basal concentration measurements of the unstimulated mast cells.

2.7. Statistical analysis

Data from the MEA are expressed in terms of (i) *spatial* (mV); i.e. field potential, (ii) *temporal* (sec); i.e. the time for the disappearance of field potential recording, and (iii) *latent period* (sec); i.e. the time from the moment of drug application to the onset of response. Where appropriate, the signal shapes, which comprise all three parameters, are shown. The measurement was obtained from an average of at least 7 randomly selected recordings from each MEA chip, which is considered as one experiment ($n = 1$). The MEA and histamine release/calcium measurement data are indicated as the mean ± S.E.M., and they were analysed using a 2-way ANOVA followed by Bonferroni *t*-tests. $P < 0.05$ was considered to indicate a statistical difference between treatment groups.

3. Results

The importance of the presence of Cl^- in anti-IgE-induced mast cell activation was revealed by studying the amount of histamine released and the extracellular electrophysiology of the activated cells. The correlation with the extent of Ca^{2+} influx during peritoneal mast cell activation by anti-IgE was further characterised using the Fura-2 fluorometric technique. The involvement of Cl^- in the mechanisms of action of DSCG and NPPB was studied and compared.

3.1. Effects of extracellular Cl^- on IgE receptor mediated mast cell activation

Anti-IgE was used to crosslink IgE molecules on the mast cell surface in a manner similar to antigens in facilitating the ligation of the IgE receptors (FcεRI) and the subsequent release of histamine. In standard buffer, anti-IgE induced a concentration-dependent increase in histamine release from 8.06 ± 2.02% (1/5,000) to 40.26 ± 2.77% (1/100, $n = 9$) from the rat peritoneal mast cell suspensions. A general inhibition of the amount of histamine released was observed from anti-IgE (1/1000 to 1/100) activated cells that had been cultured in either low Cl^- or Cl^--free buffer (Fig. 1). When compared with the controls, a significant reduction in the amount of histamine released was detected when cells were in low Cl^- buffer (0.9 ± 1.51% to 28.81 ± 3.16%, $n = 9$; $P < 0.05$), and even more so when cells were in Cl^--free buffer (−3.19 ± 0.80% to 4.08 ± 1.71%, $n = 4$, $P < 0.001$) (Fig. 1). More significant reductions in the amount of histamine released were observed in cells exposed to Cl^--free buffer than those exposed to low Cl^- buffer ($P < 0.01$).

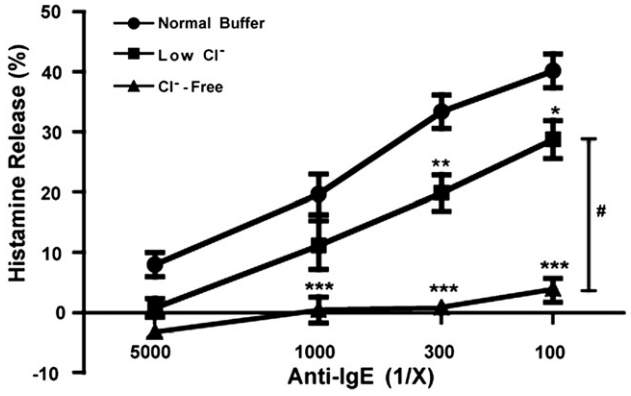

Fig. 1. Effects of anti-IgE on histamine release from rat peritoneal mast cells cultured in low Cl^- or Cl^--free buffer versus the amount released when cells were in normal buffer (*P<0.05, **P<0.01, ***P<0.001; n=4). Peritoneal mast cells were equilibrated for 10 min at 37 °C in corresponding buffers before the addition of anti-IgE (1/5000 to 1/100). More significant reductions in the amount of histamine released were observed in cells exposed to Cl^--free buffer than those exposed to low Cl^- buffer (#P<0.01; n=4). The histamine release (%) represents the percentage of total cellular histamine that has been released into the supernatant. The histamine release (%) is expressed as mean ± S.E.M.

Anti-IgE stimulated peritoneal mast cells generated extracellular electrophysiological signals (represented by the upstroke spikes), which could be due to either an influx of Cl^- or an efflux of K^+, were detected by the MEA system (Fig. 2). Spikes appeared between 21.63 ± 2.83 s and 11.83 ± 1.09 s (n=4) after anti-IgE (1/10,000–1/500) had been added, and the appearance of spikes lasted for 29.22 ± 2.40 s to 38.84 ± 5.36 s (n=4). In normal buffer, the field potential of the peritoneal mast cells reached its maximum response of 1.32 ± 0.14 mV (n=4) at 1/5000. A slight drop in field potential, albeit insignificant, was observed when anti-IgE concentration further increased to 1/500 (1.04 ± 0.06 mV, n=4) (Fig. 3A). When cells were in Cl^--free buffer, however, the recorded spikes reduced across all concentrations of anti-IgE (1/10,000 to 1/500) (Fig. 2). These spikes reduced to only negligible levels when the Cl^--free buffer was further supplemented with ChTX (Fig. 2).

Cells in low Cl^- buffer also showed a significant drop in field potential in the presence of anti-IgE but only at 1/10,000 (0.62 ± 0.21 mV, n=3, P<0.05) (Fig. 3A). While the anti-IgE stimulated peritoneal mast cells cultured in different buffers showed a general concentration-related increase in field potentials, these potentiations were significantly lower when cells were in Cl^--free buffer (1/10,000 to 1/500, n=3, P<0.05) (Fig. 3A). The lowest concentration of anti-IgE (1/50,000) elicited no effect in any buffer.

While the absence of Cl^- significantly affected the field potentials, it did not affect the temporal measurements of cells cultured in either low Cl^- or Cl^--free buffer except at the highest concentration of anti-IgE (Fig. 3B). When cells were in these buffers, the duration of response obtained at anti-IgE 1/500 was significantly lengthened (low Cl^-: 51.46 ± 5.76 s (n=3, P<0.001); Cl^--free: 46.83 ± 2.10 s (n=3, P<0.001).

Similar to the temporal measurements, the latent periods of cells were affected at the highest concentration of anti-IgE (Fig. 3C). At 1/500 anti-IgE, the latent period of cells in normal buffer was 11.83 ± 1.09 s, but this value became 22.85 ± 1.53 s (n=3; P<0.001) when cells were in low Cl^- buffer; and 22.25 ± 1.27 s (n=3; P<0.001) when cells were in Cl^--free buffer (Fig. 3C). A significant increase was also found when cells in Cl^--free buffer were exposed to anti-IgE at 1/1,000 (21.30 ± 7.61, n=3, P<0.05) (Fig. 3C).

3.2. Importance of Cl^- to the influx of Ca^{2+} in IgE receptor mediated mast cell activation

Calcium influx during peritoneal mast cell activation induced by anti-IgE was evaluated in low Cl^- or Cl^--free buffer. Although initial elevations of $[Ca^{2+}]_i$ in peritoneal mast cells were similar in either buffer, the sustained $[Ca^{2+}]_i$ levels due to Ca^{2+} influx were different.

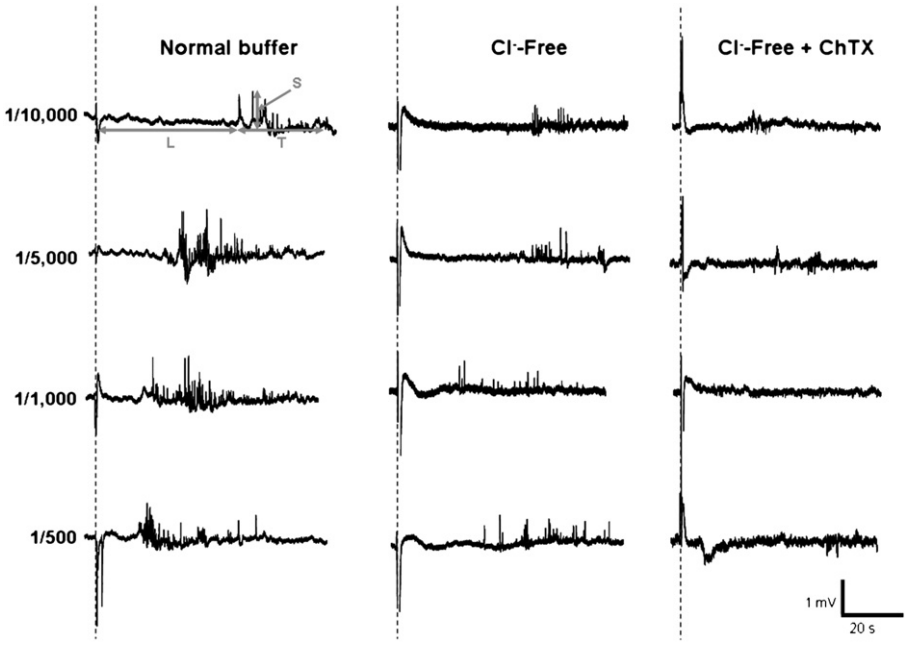

Fig. 2. Traces of field potentials triggered by anti-IgE (1/10,000 to 1/500) on rat peritoneal mast cells in normal, Cl^--free, or Cl^--free buffer containing ChTX are shown. The latent period (L), spatial (S), and temporal (T) measurements are indicated. The large artefacts along the dotted lines indicate the moment when anti-IgE was added, and the appearance of the last spike usually occurs within 70 s after the addition of anti-IgE. Since the signal elicited by anti-IgE is composed of spikes with different amplitudes, the highest spike observed corresponds to the spatial measurement; whereas the duration between the appearance of the first and the last spike is considered as the temporal measurement. The progressive reduction in field potentials in Cl^--free buffer or Cl^--free buffer containing ChTX indicates that the measured positive spikes were composed of both Cl^- and K^+ (signal strengths: normal buffer>Cl^--free buffer>Cl^--free buffer containing ChTX).

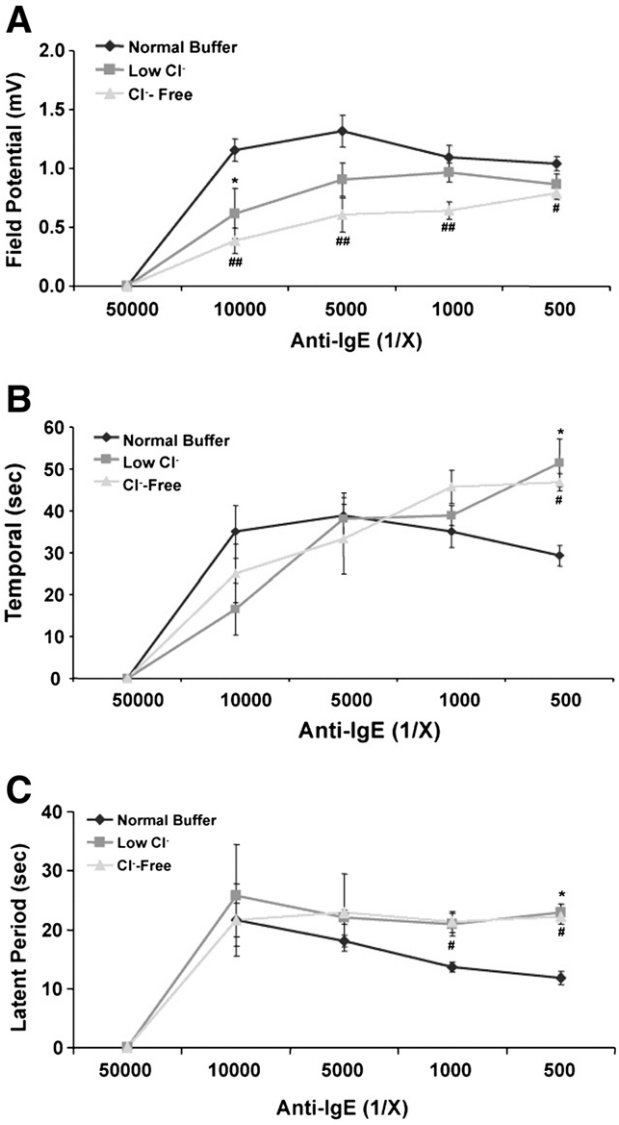

Fig. 3. Effects of anti-IgE (1/50,000 to 1/500) on rat peritoneal mast cells cultured in normal, low Cl^-, or Cl^--free buffer in terms of (A) field potentials, (B) temporal measurements, and (C) latent periods are shown. No signals were observed at the lowest anti-IgE concentration (1/50,000) regardless of the type of buffer used. (a) The field potentials of cells cultured in low Cl^- buffer ($n=3$) or Cl^--free buffer ($n=3$) were significantly reduced versus the values obtained when cells were in normal buffer ($n=4$). At the highest anti-IgE concentration (1/500), the temporal measurements (b) and the latent periods (c) were increased significantly when cells were in low Cl^- or Cl^--free buffer. The field potentials are expressed as mV ± S.E.M., and the temporal and latent measurements are expressed as second ± S.E.M. (Normal vs Low Cl^-, $^*P<0.05$; normal vs Cl^--free, $^{\#}P<0.05$, $^{\#\#}P<0.01$).

The total amount of Ca^{2+} entering the cells was much lower when the Cl^--free buffer was used. Compared with cells cultured in normal buffer, there were approximately 30% and 70% reductions in Ca^{2+} influx with cells cultured in low Cl^- ($n=4$) and Cl^--free buffer ($n=4$), respectively (Fig. 4).

3.3. Comparison between the effects of NPPB and DSCG on IgE receptor mediated mast cell activation

NPPB is a potent chloride channel blocker that inhibits the amount of histamine released from the rat peritoneal mast cells. The inhibitory effect of NPPB (10 μM) on cells with or without 10 min pre-incubation of anti-IgE (1/5,000–1/100) was similar (Fig. 5A). The maximal inhibition by NPPB was observed when the lowest concentration of anti-IgE

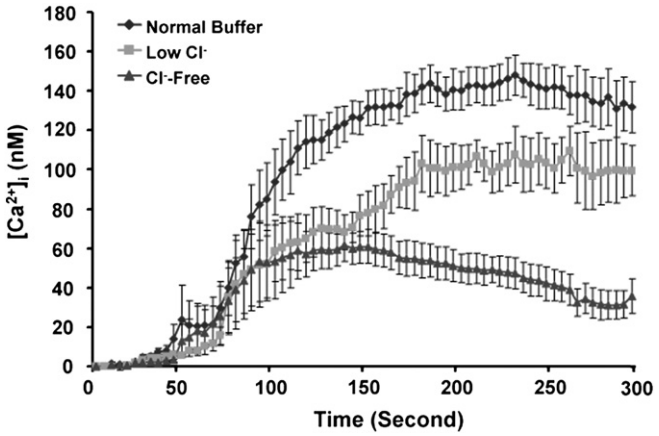

Fig. 4. Effects of anti-IgE on the changes in free intracellular Ca^{2+} content in Fura-2 loaded rat peritoneal mast cells. The results from peritoneal mast cells cultured in normal, low Cl^-, or Cl^--free buffer were compared. Anti-IgE at a dilution of 1/200 was added to the peritoneal mast cells at 50 s. Values are the mean of 4 experiments, with an averaged value of 20 cells from each experiment. The intracellular Ca^{2+} content is expressed as nM ± S.E.M. Significant inhibition *(P<0.05)* of the intracellular Ca^{2+} content by the lowering of Cl^- content (low Cl^- and Cl^--free) was observed after 100 s.

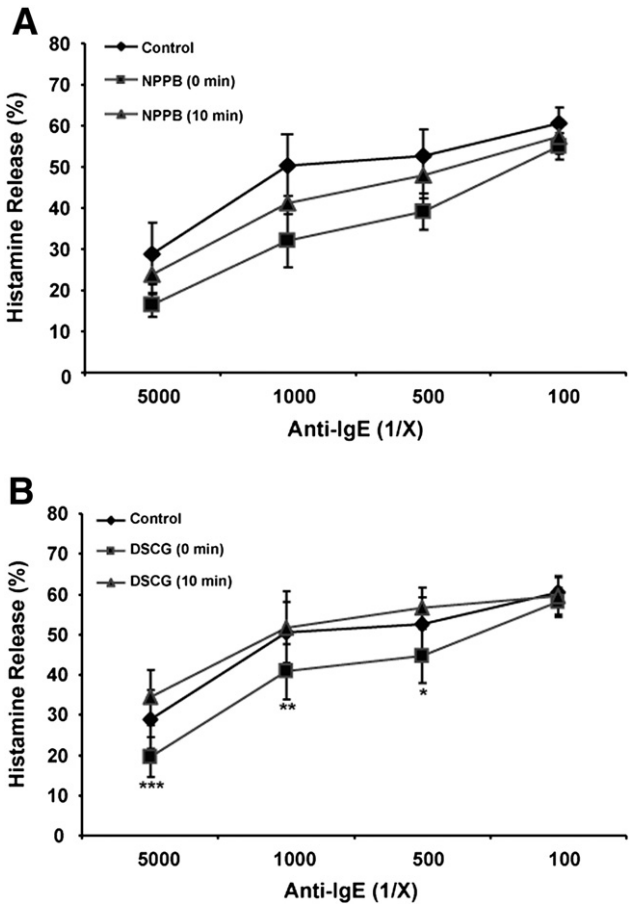

Fig. 5. Effects of anti-IgE on the amount of histamine released from rat peritoneal mast cells cultured in normal buffer containing NPPB (A) or DSCG (B). Peritoneal mast cells were equilibrated in normal buffer containing either NPPB (10 μM) or DSCG (100 μM), with or without 10 min pre-incubation, before the addition of anti-IgE (1/5,000 to 1/100). Reductions in anti-IgE stimulated histamine release by NPPB were observed in both pre-incubation times, while a reduction in histamine release was only observed in anti-IgE activated cells without DSCG pre-incubation (inhibition at 0 min vs 10 min: $^*P<0.05$, $^{**}P<0.01$, $^{***}P<0.001$; $n=4$). The histamine release (%) represents the percentage of total cellular histamine that has been released into the supernatant. The histamine release (%) is expressed as mean ± S.E.M.

(1/5,000) was used. The extent of these reductions was not significant between cells that had been incubated for 10 min (32.59 ± 5.85%, $n = 3$) and those without (46.41 ± 3.25%, $n = 3$).

Anti-IgE-induced histamine release was inhibited, particularly effective at the lowest concentration of 1/5,000, by the simultaneous presence of DSCG (100 μM), causing a 37.81 ± 11.23% ($n = 3$, Fig. 5B) reduction. But this inhibition on histamine release was significantly diminished when cells were pre-incubated with DSCG for 10 min prior to the addition of anti-IgE, with the maximal inhibition being observed at 1/1,000 (−3.86 ± 3.69%, $n = 3$, $P<0.05$).

A complete inhibition of anti-IgE (1/5,000–1/500) elicited field potentials by NPPB (10 μM), with or without 10 min incubation, was observed (Fig. 6A). NPPB was still effective at blocking the effect of the highest concentration of anti-IgE (1/100, $P<0.05$). DSCG (100 μM), regardless of the incubation period (0 or 10 min), significantly suppressed the anti-IgE activated field potentials to the same extent (Fig. 6B).

4. Discussion

The involvement of Ca^{2+} in mast cell activation has been characterised extensively [4,5,25]. Besides Ca^{2+} influx, movements of other ions in both resting and activated mast cells have also been reported [15,16,26]. For example, evidence suggests the movement of Cl^- and K^+ may also participate in the activation process [15,16]. Indeed, studies have shown that Cl^- channel openers and blockers can affect mediators release from activated mast cells [10,12,13].

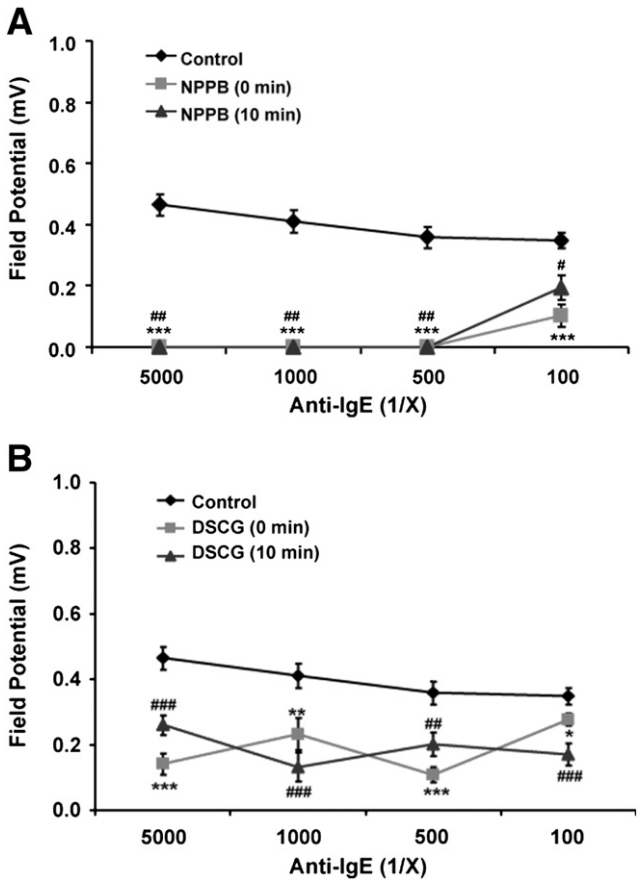

Fig. 6. Effects of anti-IgE (1/5000 to 1/100) on rat peritoneal mast cells cultured in normal buffer containing NPPB (6A) or DSCG (6B) in terms of field potentials are shown. Both NPPB (10 μM) and DSCG (100 μM), with or without 10 min pre-incubation, significantly inhibited the field potentials across all concentrations of anti-IgE. The field potentials are expressed as mV ± S.E.M. (0 min pre-incubation $^*P<0.05$, $^{**}P<0.01$, $^{***}P<0.001$; 10 min pre-incubation $^{\#}P<0.05$, $^{\#\#}P<0.01$, $^{\#\#\#}P<0.01$; $n = 3$).

Furthermore, the inhibitory effect of DSCG, a mast cell stabiliser, on mast cell activation has been related to the prevention of Ca^{2+} influx by indirectly blocking Cl^- channels [21]. In the present study, the effects of Cl^- concentration using modified buffers and in the presence of NPPB on mast cell activation were compared with data obtained using DSCG. A substantial inhibition of the release of histamine was observed when the antigen-stimulated peritoneal mast cells were cultured in low Cl^- or Cl^--free buffer (Fig. 1), indicating the significance of Cl^- in the degranulation process. Complete inhibition of histamine release was observed when the lowest concentration of anti-IgE (1/3,000) was used to challenge the mast cells that were cultured in complete Cl^--free solution. The negative values obtained were probably due to the inconsistent histamine release at the basal level when the cells were not being activated. Following the first use of MEA in measuring the physiological responses of mast cells in our laboratory [27], the present study further demonstrates that it could be used as a new means to measuring these electrophysiological changes by elucidating some well established responses of mast cells under activation. In the present study, dominant field potential positive spikes induced by anti-IgE in rat peritoneal mast cells appeared after a delay of 10–20 sec (Fig. 2). The positive field potential change could represent either an inward anionic current or an outward cationic current [28]. In order to verify the involvement of a particular type of ions during mast cell activation, buffers deficient in different ions of interest were used. The reduction in positive field potentials spikes when the cells were cultured in Cl^--free buffer (Figs. 2 and 3A) and the disappearance of the remaining spikes in Cl^--free buffer containing ChTX demonstrated that movements of both Cl^- and K^+ were involved in the anti-IgE stimulated peritoneal mast cell activation process, and that the efflux of K^+ was chiefly via the K_{Ca} channels (Fig. 2). In the present study, there were no significant changes in exFP amplitude with increasing concentrations of anti-IgE. The exFP amplitude was maintained at a range of 1.04 ± 0.06 mV to 1.32 ± 0.14 mV ($n = 4$). As we reduced the anti-IgE concentration to 1/50,000, both histamine release and exFP were not detected. It is possible that a threshold level is required for maintaining the hyperpolarised state for further mast cell degranulation.

The delayed Cl^- current is characterised by a slow onset time and a long activation process, and this current can be activated by the application of intracellular cAMP [18]. Recently, functional cystic fibrosis transmembrane conductance regulator (CFTR), a cAMP-regulated Cl^- channel, has been identified in rat peritoneal mast cells [29]. The cAMP-induced Cl^- current in peritoneal mast cells tends to appear within 10–30 s of antigen-induced activation, which is in good agreement with the onset time of positive spikes found in the present study (cells in normal buffer, 11.83 ± 1.09 to 21.63 ± 2.83 s). There is also another study that suggests the slow Cl^- current via CFTR may involve the release of newly synthesised mast cell mediators, and this would explain the late appearance of Cl^- conductance during mast cell degranulation [16].

During mast cell activation, several ion-induced currents including I_{CRAC} [30], slowly outwardly rectifying chloride [18], calcium activated chloride [16], and calcium activated potassium currents [31,32] have been observed. Amongst the identified ionic currents, the I_{CRAC} is the most important as it is responsible for mast cell degranulation. The CRAC, which carries Ca^{2+} into cells, conducts larger currents at more hyperpolarising potentials [30]. Movements of Cl^- and K^+ therefore maintain a hyperpolarised mast cell membrane, modulate Ca^{2+} influx, and further enhance mast cell degranulation [33].

There are two phases of $[Ca^{2+}]_i$ elevation during mast cell activation following cross-linking of FcεRI: an initial phase, which is due to inositol 1,4,5-triphosphate-dependent release of $[Ca^{2+}]_i$ from the internal Ca^{2+} store; and a sustained phase, which is due to the influx of Ca^{2+} via the activated CRAC [5,30,34,35]. Based on the $[Ca^{2+}]_i$ measurements obtained, a reduction in the sustained $[Ca^{2+}]_i$ levels, which represent the influx of Ca^{2+}, in Cl^--depleted buffers during antigen-stimulated

peritoneal mast cell activation (Fig. 4) suggests that extracellular Cl^- ions play a crucial role in modulating the extent of Ca^{2+} influx.

The presence of NPPB (with or without 10 min pre-incubation) inhibited the amount of histamine released and the extracellular field potentials from the anti-IgE activated cells (Fig. 5A and Fig. 6A, respectively). The inhibition of histamine release by NPPB, however, was less effective when compared with the amount released by the complete removal of extracellular Cl^- in buffer, where nearly 100% was achieved (Fig. 1). Since NPPB has been reported to block the delayed Cl^- current in mast cells [18], the insufficient blocking of Cl^- by NPPB suggests that other Cl^- channels on mast cells might also be involved during anti-IgE activation. The mast cell stabiliser DSCG has also been suggested to play an inhibitory role in mast cell activation via an indirect blockade of Cl^- channels [21]. In this study, DSCG could only inhibit the amount of histamine released without pre-incubation. In fact, a 10 min pre-incubation of DSCG with cells prior to the stimulation of anti-IgE abolished its inhibitory influence (Fig. 5B). The inhibiting effect of DSCG on anti-IgE activated mast cells demonstrated tachyphylaxis; i.e. a rapid loss of activity following incubation with cells [36]. Since the extracellular field potential changes induced by anti-IgE were chiefly due to Cl^- influx (Fig. 2), we used that as a reference to compare to the field potential changes of activated mast cells in the presence of DSCG. The field potentials were reduced in anti-IgE activated mast cells with or without 10 min incubation (Fig. 6B), indicating that the influx of Cl^- was blocked by DSCG. However, the amount of histamine released was not suppressed by pre-incubating the cells with DSCG for 10 min (Fig. 5B). These results suggest that the suppression of Cl^- influx might not be sufficient to account for the inhibitory action of DSCG on anti-IgE activated mast cells. Recently, DSCG has been shown to be a potent G-protein-coupled receptor 35 (GPR35) agonist on rat mast cells [37]. The GPR35 is coupled to G_i signalling pathway, which involves the release of Ca^{2+} from intracellular stores [38]. While the transient elevation of $[Ca^{2+}]_i$ may not be sufficient to trigger degranulation; however, the activation of phospholipase C (PLC) and phosphoinositide 3-kinase (PI3K) by the G_i-coupled receptor and FcεRI provides a possible mechanism by which the signals induced by these receptors may be integrated for the synergistic enhancement of mast cell degranulation [39]. The mechanism of this synergy is still unclear, but enhancement of antigen-induced $[Ca^{2+}]_i$ modulation has been observed [39]. This overall $[Ca^{2+}]_i$ elevation may be sufficient to induce mast cell degranulation by overcoming the partial inhibitory effect of DSCG on Cl^- influx.

In the current extracellular electrophysiological study, the whole signal shape as well as the onset and completion time of the anti-IgE induced effect is completely different from those obtained in a previous study using compound 48/80 [27]. This is because anti-IgE and compound 48/80 are known to activate mast cells via two distinct mechanisms [39]. Mast cell degranulation by anti-IgE depends on the presence of extracellular Ca^{2+}, while compound 48/80 activated degranulation does not [40]. Compound 48/80 induces mast cell degranulation by activating PLC and releasing Ca^{2+} from intracellular store. The K_{ca} channels further hyperpolarise the cell membrane and enhance mast cell degranulation. The efflux of K^+ across the cell membrane was detected using the MEA in our previous study [27]. In order to maintain a hyperpolarisation state, which favours the influx of Ca^{2+} during anti-IgE activation of the mast cell membrane, the influx of Cl^- becomes significantly more important. The differences and the relative importance of Cl^- influx via anti-IgE or compound 48/80 induced mast cell activation have been carried out by other groups [10,41], and their results are in line with the present MEA study. In the case of compound 48/80 stimulated mast cells, a stronger field potential (4–6 mV) is elicited by the activation of inwardly rectifying K^+ and K_{Ca} channels, thus the membrane potential is hyperpolarised rapidly and this explains the shorter onset (2–4 s) and response (1–6 s) timeframe when compared to the anti-IgE response observed in the present study. The significant differences in the detected signals further demonstrate the feasibility of using the MEA system to study different activation pathways of non-spontaneously active cells. It is important to bear in mind that these recorded signals are the resultant changes of a number of ions as opposed to the more traditional patch-clamp studies where a single channel conductance is measured. The application of patch-clamp in the study of mast cell electrophysiology is based on the assumption that the estimation of secretory activity of a single cell can be quantified by the cell membrane capacitance. Since one of the principles of the MEA is based on capacitive coupling between the cell and the electrode and this is then subsequently interpreted as field potentials based on the point contact model, the changes in field potentials can thus be used to correlate with the activation of these immunological cells. The benefits of using the MEA over the conventional patch-clamp technique included simultaneous recording of signals from 64 individual cells on a single chip and the experiments are quick and easy to perform [27]. Also, by comparing the time course of anti-IgE mediated field potential change of mast cells (< 70 s) with the time it takes histamine to release (> 4 min) [42], it seems clear that electrophysiological events must take place before the degranulation process. These “signal shapes” of different activating agents provide a “physiological signature” that may be used for the profiling or the characterisation of mast cells under different conditions. Together with the NPPB and DSCG results from the present study, we can foresee the feasibility of using the present MEA system for the screening of ion-channel modulators that are potentially anti-allergic agents. The ability to identify different types of ions in mast cell activation is especially important for the study of neuroimmunology when considering the role of ionic channels as targets for neurotransmitter action in mast cell activation [43].

5. Conclusions

The results obtained from the MEA are in good agreement with the current knowledge of electrophysiology of mast cells undergoing degranulation following immunological challenge. While the MEA cannot yield information about single channel properties, it is much more convenient to use than the patch-clamp and can provide information on the global changes in electrophysiological responses of non-excitable cells rapidly.

Acknowledgments

This work is supported by an Earmarked Grant from the Research Grant Council of Hong Kong under the contract number 611205 (awarded to M. Chan, HKUST) and Helmholtz Association of National Research Centres, Germany. The authors would like to thank N. Wolters (IBN-2, Electronic Workshop) and Y. Zhang (IBN-2) for their technical expertise in designing the current MEA system. MEA chips were fabricated by M. Krause in a previous project at the Max-Planck-Institute for Polymer Research, Mainz, Germany, within the group of Wolfgang Knoll.

References

[1] J.M. Oliver, C.L. Kepley, E. Ortega, B.S. Wilson, Immunologically mediated signaling in basophils and mast cells: finding therapeutic targets for allergic diseases in the human FcvarepsilonR1 signaling pathway, Immunopharmacology 48 (2000) 269–281.
[2] J. Rivera, A. Olivera, A current understanding of Fc epsilon RI-dependent mast cell activation, Curr. Allergy Asthma Rep. 8 (2008) 14–20.
[3] A.M. Gilfillan, C. Tkaczyk, Integrated signalling pathways for mast-cell activation, Nat. Rev. Immunol. 6 (2006) 218–230.
[4] R. Penner, E. Neher, The role of calcium in stimulus-secretion coupling in excitable and non-excitable cells, J. Exp. Biol. 139 (1988) 329–345.
[5] W.C. Chang, Store-operated calcium channels and pro-inflammatory signals, Acta Pharmacol. Sin. 27 (2006) 813–820.

[6] S.M. Duffy, G. Cruse, W.J. Lawley, P. Bradding, Beta2-adrenoceptor regulation of the K+ channel iKCa1 in human mast cells, FASEB J. 19 (2005) 1006–1008.
[7] S.M. Duffy, P. Berger, G. Cruse, W. Yang, S.J. Bolton, P. Bradding, The K+ channel iKCA1 potentiates Ca2+ influx and degranulation in human lung mast cells, J. Allergy Clin. Immunol. 114 (2004) 66–72.
[8] A. Nemeth, P. Magyar, R. Herceg, A. Huszti, Potassium-induced histamine release from mast cells and its inhibition by ketotifen, Agents Actions 20 (1987) 149–152.
[9] Y.X. Qian, M.A. McCloskey, Activation of mast cell K+ channels through multiple G protein-linked receptors, Proc. Natl. Acad. Sci. U.S.A. 90 (1993) 7844–7848.
[10] J. Dietrich, M. Lindau, Chloride channels in mast cells: block by DIDS and role in exocytosis, J. Gen. Physiol. 104 (1994) 1099–1111.
[11] A. Nemeth, P. Magyar, Z. Huszti, Inhibition of potassium-induced release of histamine from mast cells by tetraethylammonium and tetramethylammonium, Agents Actions 30 (1990) 143–145.
[12] M. Reinsprecht, M.H. Rohn, R.J. Spadinger, I. Pecht, H. Schindler, C. Romanin, Blockade of capacitive Ca2+ influx by Cl- channel blockers inhibits secretion from rat mucosal-type mast cells, Mol. Pharmacol. 47 (1995) 1014–1020.
[13] C. Romanin, M. Reinsprecht, I. Pecht, H. Schindler, Immunologically activated chloride channels involved in degranulation of rat mucosal mast cells. EMBO J. 10 (1991) 3603–3608.
[14] A.B. Parekh, H. Terlau, W. Stuhmer, Depletion of InsP3 stores activates a Ca2+ and K+ current by means of a phosphatase and a diffusible messenger, Nature 364 (1993) 814–818.
[15] P. Bradding, E.C. Conley, Human mast cell ion channels, Clin. Exp. Allergy 32 (2002) 979–983.
[16] P. Bradding, Mast cell ion channels, Chem. Immunol. Allergy 87 (2005) 163–178.
[17] P.B. Hill, R.J. Martin, H.R. Miller, Characterization of whole-cell currents in mucosal and connective tissue rat mast cells using amphotericin-B-perforated patches and temperature control, Pflugers Arch. 432 (1996) 986–994.
[18] G. Matthews, E. Neher, R. Penner, Chloride conductance activated by external agonists and internal messengers in rat peritoneal mast cells, J. Physiol. 418 (1989) 131–144.
[19] R. Penner, G. Matthews, E. Neher, Regulation of calcium influx by second messengers in rat mast cells, Nature 334 (1988) 499–504.
[20] J. Seebeck, S. Tritschler, T. Roloff, M.L. Kruse, W.E. Schmidt, A. Ziegler, The outwardly rectifying chloride channel in rat peritoneal mast cells is regulated by serine/threonine kinases and phosphatases, Pflugers Arch. 443 (2002) 558–564.
[21] A.A. Norris, E.W. Alton, Chloride transport and the action of sodium cromoglycate and nedocromil sodium in asthma. Clin. Exp. Allergy 26 (1996) 250–253.
[22] H. Ecken, S. Ingebrandt, M. Krause, D. Richter, M. Hara, A. Offenhäusser, 64-Channel extended gate electrode arrays for extracellular signal recording, Electrochimica Acta 48 (2003) 3355–3362.
[23] M. Krause, S. Ingebrandt, D. Richter, M. Denyer, M. Scholl, C. Sprossler, A. Offenhausser, Extended gate electrode arrays for extracellular signal recordings Sensors and Actuators B: Chemical, 70, 2000, pp. 101–107.
[24] G. Grynkiewicz, M. Poenie, R.Y. Tsien, A new generation of Ca2+ indicators with greatly improved fluorescence properties, J. Biol. Chem. 260 (1985) 3440–3450.
[25] R. Penner, E. Neher, Secretory responses of rat peritoneal mast cells to high intracellular calcium, FEBS Lett. 226 (1988) 307–313.
[26] S.M. Duffy, W.J. Lawley, E.C. Conley, P. Bradding, Resting and activation-dependent ion channels in human mast cells, J. Immunol. 167 (2001) 4261–4270.
[27] C.K. Yeung, J.K. Law, S.W. Sam, S. Ingebrandt, H.Y. Lau, J.A. Rudd, M. Chan, The use of microelectrode array (MEA) to study rat peritoneal mast cell activation, J. Pharmacol. Sci. 107 (2008) 201–212.
[28] S. Ingebrandt, C.K. Yeung, M. Krause, A. Offenhausser, Neuron-transistor coupling: interpretation of individual extracellular recorded signals, Eur. Biophys. J. 34 (2005) 144–154.
[29] M. Kulka, M. Gilchrist, M. Duszyk, A.D. Befus, Expression and functional characterization of CFTR in mast cells, J. Leukoc. Biol. 71 (2002) 54–64.
[30] M. Hoth, R. Penner, Calcium release-activated calcium current in rat mast cells, J. Physiol. 465 (1993) 359–386.
[31] M. Gericke, O. Dar, G. Droogmans, I. Pecht, B. Nilius, Immunological stimulation of single rat basophilic leukemia RBL-2H3 cells co-activates Ca(2+)-entry and K(+)-channels, Cell Calcium 17 (1995) 71–83.
[32] M. Hoth, Depletion of intracellular calcium stores activates an outward potassium current in mast and RBL-1 cells that is correlated with CRAC channel activation, FEBS Lett. 390 (1996) 285–288.
[33] A.G. Cabado, S. Despa, M.A. Botana, M.R. Vieytes, M. Gonzalez, L.M. Botana, Membrane potential changes associated with calcium signals in human lymphocytes and rat mast cells, Life Sci. 64 (1999) 681–696.
[34] J.C. Foreman, J.L. Mongar, B.D. Gomperts, Calcium ionophores and movement of calcium ions following the physiological stimulus to a secretory process, Nature 245 (1973) 249–251.
[35] R. Penner, C. Fasolato, M. Hoth, Calcium influx and its control by calcium release, Curr. Opin. Neurobiol. 3 (1993) 368–374.
[36] C.P. Sung, H.L. Saunders, R.D. Krell, L.W. Chakrin, Studies on the mechanism of tachyphylaxis to disodium cromoglycate, Int. Arch. Allergy Appl. Immunol. 55 (1977) 374–384.
[37] Y. Yang, J.Y. Lu, X. Wu, S. Summer, J. Whoriskey, C. Saris, J.D. Reagan, G-protein-coupled receptor 35 is a target of the asthma drugs cromolyn disodium and nedocromil sodium, Pharmacology 86 (2010) 1–5.
[38] J. Senyshyn, R.A. Baumgartner, M.A. Beaven, Quercetin sensitizes RBL-2H3 cells to polybasic mast cell secretagogues through increased expression of Gi GTP-binding proteins linked to a phospholipase C signaling pathway, J. Immunol. 160 (1998) 5136–5144.
[39] H.S. Kuehn, A.M. Gilfillan, G protein-coupled receptors and the modification of FcepsilonRI-mediated mast cell activation, Immunol. Lett. 113 (2007) 59–69.
[40] T. Roloff, N. Wordehoff, A. Ziegler, J. Seebeck, Evidence against the functional involvement of outwardly rectifying Cl- channels in agonist-induced mast cell exocytosis, Eur. J. Pharmacol. 431 (2001) 1–9.
[41] A.C. Redrup, J.C. Foreman, H.A. Hayes, F.L. Pearce, Fc epsilon RI-mediated chloride uptake by rat mast cells: modulation by chloride transport inhibitors in relation to histamine secretion, Br. J. Pharmacol. 122 (1997) 1188–1194.
[42] M. Takei, M. Ueno, K. Endo, Role of intracellular Ca2+ on histamine release from rat peritoneal mast cells, J. Pharm. Sci. 81 (1992) 518–520.
[43] J. Janiszewski, J.D. Huizinga, M.G. Blennerhassett, Mast cell ionic channels: significance for stimulus-secretion coupling, Can. J. Physiol. Pharmacol. 70 (1992) 1–7.